

NONLINEAR DYNAMICS OF A FLEXIBLE BEAM IN A CENTRAL GRAVITATIONAL FIELD—II. NONLINEAR MOTIONS IN CIRCULAR ORBIT

MARCELO R. M. CRESPO DA SILVA and CLIFFORD L. ZARETZKY
Department of Mechanical Engineering, Aeronautical Engineering and Mechanics,
Rensselaer Polytechnic Institute, Troy, NY 12180-3590, U.S.A.

(Received 7 December 1992; in revised form 19 March 1993)

Abstract—The coupled nonlinear pitch-bending response of a free-free beam in a circular orbit, when the beam is subjected to a periodic external excitation, is analysed. The nonlinearities present in the differential equations of motion are due to deformation of the beam (i.e. curvature and inertia nonlinearities) and to the gravity-gradient moments. Perturbation methods are used to analyse the motion. Several resonant motions exhibited by the system are analysed in detail, namely, harmonic resonances when the frequency of the external excitation, Ω , is either near the natural frequency of the flexural or of the pitch motion, and a superharmonic resonance when Ω is near one half of the natural frequency of the pitch motion. The latter two resonances are associated with very low excitation frequencies.

INTRODUCTION

The nonlinear differential equations governing the coupled flexural-pitching motions of a beam subjected to the gravity-gradient moments due to a central attracting massive body were formulated by Crespo da Silva and Zaretzky (1993). The beam may also be subjected to external forces other than those due to the gravity-gradient. The equations developed by the authors (Crespo da Silva and Zaretzky, 1993) contain the effect of all the geometric nonlinearities in the system. In order to be able to investigate the motion by analytical techniques, the full nonlinear differential equations of motion were also expanded for “moderate” motions to contain polynomial nonlinearities in terms of the dependent variables. For this, a circular orbit was considered in Crespo da Silva and Zaretzky (1993), and all the nonlinearities up to third-order in a bookkeeping parameter ϵ , which is introduced only to keep track of orders of smallness, were retained in the resulting integro-partial differential equations. Galerkin’s procedure was subsequently applied to the latter equations using the eigenmodes for the orbiting beam as the basis for the modal reduction.

In this paper, the coupled nonlinear flexural-pitching motions of a free-free beam in circular orbit are investigated. For this, eqns (38) and (40) in Crespo da Silva and Zaretzky (1993) are used for the analysis. As indicated above, the $O(\epsilon^3)$ nonlinearities contained in those equations include those due to deformation of the beam, which consist of inertia and curvature nonlinearities. A uniform beam with constant distributed properties along its span is considered in the present analysis.

ANALYSIS OF THE MOTION

The system considered here consists of a free-free homogeneous beam of length L and constant specific mass $m \text{ Kg m}^{-1}$, and stiffness $D_c \text{ N m}^2$, whose center of mass C is in a circular orbit around a center of attraction E . As shown in Fig. 1, the motion is described in terms of the elastic deformation $v(s, t)$ (normalized by the length of the beam) and of the pitch angle $\theta(t)$ between the “local vertical” and a principal axis of the deformed beam. The quantities s and t are, respectively, arc-length along the beam, normalized by L , and normalized time. The variables and nomenclature used here are the same as those used by Crespo da Silva and Zaretzky (1993). Let the beam be subjected to a distributed periodic force $F_\eta(s, t) = E_\eta(s) \cos(\Omega t)$ applied along the $\hat{\eta}$ direction shown in Fig. 1. With $v(s, t)$ approximated as $v(s, t) = F(s)v_\eta(t)$, and dots used to denote differentiation with respect to

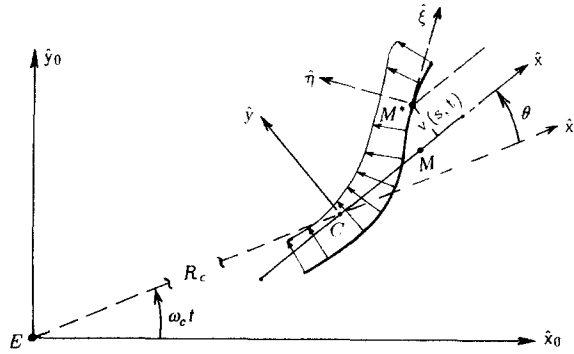


Fig. 1. Free-free beam in circular orbit.

normalized time t , the $O(\varepsilon^3)$ normalized differential equations of motion, obtained directly from eqns (38) and (40) in Crespo da Silva and Zaretzky (1993), are

$$\ddot{v}_t + c\dot{v}_t + \omega^2 v_t + (\beta_1 - 1)(2\omega_c + \dot{\theta})\dot{\theta}v_t - 3\omega_c^2(\beta_1 + 1)\theta^2 v_t + \beta_2 v_t (v_t^2)'' + \beta_3 v_t^3 = f_t \cos(\Omega t) + v_t^2 f_{v_t} \cos(\Omega t), \quad (1)$$

$$\ddot{\theta} + 3\omega_c^2 \theta - 2\omega_c^2 \theta^3 - 12\beta_1 [v_t^2 (\ddot{\theta} + 3\omega_c^2 \theta) + (\omega_c + \dot{\theta})(v_t^2)'] + 12[(\omega_c + \dot{\theta})v_t^2] - 36\omega_c^2 v_t^2 \theta = f_\theta \cos(\Omega t) + v_t^2 f_{\theta t} \cos(\Omega t). \quad (2)$$

The full nonlinear differential equations of motion were expanded so that perturbation methods can be used to analyse the motion. In eqns (1) and (2), c is a structural damping coefficient, normalized by $L^2/\sqrt{mD_\zeta}$, ω is the undamped natural frequency for the flexural motion and ω_c is the angular speed of the circular orbit of the beam's mass center, both normalized by the quantity $L^2\sqrt{m/D_\zeta}$. The quantities β_1 , β_2 and β_3 are Galerkin coefficients defined in Crespo da Silva and Zaretzky (1993). The eigenfunction $F(s)$ and the natural frequency ω are obtained numerically by solving the following differential equation iteratively (Crespo da Silva *et al.*, 1991) with the boundary condition $F'''(0) = F'''(1) = F''(0) = F''(1) = 0$:

$$F'''' - \omega^2 F + \frac{3}{2}\omega_c^2 [(s^2 - s)F']' = 0. \quad (3)$$

The values of the constants ω , β_1 , β_2 and β_3 , for the first mode, are given in Table 1 for several values of ω_c . Note that for $0 < \omega_c \leq 1$ the values of the constants shown are within 1% of their values for the limiting case $\omega_c = 0$ (which corresponds to a free-free beam that is not in orbit, as found in classical structural mechanics textbooks). These numerical values are used later in this paper to generate a number of results to illustrate the coupled flexural-pitching motion of the orbiting beam. It is of interest to notice that for a 100 m long aluminum hollow rectangular (or circular) beam with small wall thickness and with $E = 73 \times 10^9 \text{ N m}^{-2}$, $\rho = 2.77 \text{ g cm}^{-3}$ (AL2024-T4) and cross-sectional dimensions of $29 \times 29 \text{ cm}$ (or 29 cm in diameter for the hollow circular cross-section) one obtains $\omega_c \approx 0.02$ for a shallow Earth orbit whose orbital period is approximately 86.4 min. The value of ω_c becomes 100 times larger if the beam's length is increased to 1000 m. As indicated in Table

Table 1. Values of ω , β_1 , β_2 and β_3 for the first mode of a beam in circular orbit

ω_c	ω	β_1	β_2	β_3
0	22.373	3.0498	61.2	20,581
0.02	22.373	3.0498	61.2	20,581
1	22.577	3.0496	61.2	20,689
5	27.03	3.0463	61.208	23,306

1, for small values of ω_c , the values obtained for ω and for the constants β_1, β_2 and β_3 , are essentially the same as those for the nonorbiting beam.

The quantities $f_v, f_{v\eta}, f_\theta$ and $f_{\theta\eta}$ that appear in eqns (1) and (2) are defined by eqns (4a–d) given below. The quantity $K_2(s)$ that appears in eqn (4d) is defined as

$$K_2(s) = \left[\int_s^1 F'^2 ds - \int_0^1 sF'^2 ds \right] / 2:$$

$$f_v = \int_0^1 F(s)E_\eta(s) ds, \tag{4a}$$

$$f_{v\eta} = \int_0^1 F(s) \left[F''(s) \int_1^s F'(s)E_\eta(s) ds + \frac{1}{2}F'^2(s)E_\eta(s) \right] ds, \tag{4b}$$

$$f_\theta = 12 \int_0^1 (s - \frac{1}{2})E_\eta(s) ds, \tag{4c}$$

$$f_{\theta\eta} = 12 \int_0^1 [K_2(s) + F(s)F'(s) - \frac{1}{2}(s - \frac{1}{2})F'^2(s)]E_\eta(s) ds. \tag{4d}$$

Table 2 shows the corresponding values of $f_v, f_{v\eta}, f_\theta$ and $f_{\theta\eta}$ for several illustrative functions $E_\eta(s)$, with $F(s)$ equal to the eigenfunction for the first bending mode and $0 \leq \omega_c \leq 1$. All the values equal to 0 or 1 in that table were calculated analytically while the other values were determined by evaluating eqns (4a–d) numerically.

Equations (1) and (2) exhibit a number of resonance conditions involving the natural frequencies ω and $\omega_\theta = \sqrt{3}\omega_c$, and the frequency Ω of the external excitation. These include the internal resonances $\omega_\theta \approx \omega$ and $\omega_\theta \approx 2\omega$. However, as indicated in Crespo da Silva and Zaretsky (1993), and illustrated in Table 1, these internal resonances are not physically possible due to the fact that $\omega > \omega_\theta$. Here, the harmonic nonlinear resonant responses when the frequency of the external excitation, Ω , is either near ω or near ω_θ , and the superharmonic resonance where Ω is near $\omega_\theta/2$, are investigated in detail.

To analyse the coupled motions governed by eqns (1) and (2), we introduce an arbitrary small parameter ϵ that is only used to keep track of the different orders of approximation. An approximate solution to the equations of motion is sought in terms of a power series in ϵ . The method of multiple time scales (Nayfeh and Mook, 1989) will be used to generate solutions that are valid for arbitrarily large values of time. For the $O(\epsilon^3)$ differential equations, the time scales $t_0 = t, t_1 = \epsilon t$ and $t_2 = \epsilon^2 t$ are needed. The generalized coordinates $v_i(t)$ and $\theta(t)$ are expressed as

$$v_i(t_0, t_1, t_2; \epsilon) = \epsilon v_{i1}(t_0, t_1, t_2) + \epsilon^2 v_{i2}(t_0, t_1, t_2) + \epsilon^3 v_{i3}(t_0, t_1, t_2) + \dots, \tag{5a}$$

$$\theta(t_0, t_1, t_2; \epsilon) = \epsilon \theta_1(t_0, t_1, t_2) + \epsilon^2 \theta_2(t_0, t_1, t_2) + \epsilon^3 \theta_3(t_0, t_1, t_2) + \dots \tag{5b}$$

and the structural damping coefficient c is treated as a small quantity and transferred out of the $O(\epsilon)$ equation by letting

Table 2. Values of $f_v, f_{v\eta}, f_\theta$ and $f_{\theta\eta}$ for $0 \leq \omega_c \leq 1$ and ω for the first bending mode

$E_\eta(s)$	f_v	$f_{v\eta}$	f_θ	$f_{\theta\eta}$
$F(s)$	1	44.96	0	$6.07 \times 10^{-7} \approx 0$
1	0	-54.34	0	≈ 0
$s - \frac{1}{2}$	0	-12.3	1	-37.9
$(s - \frac{1}{2})^2$	-0.07427	-7.87	0	≈ 0
s^2	-0.07427	-33.76	1	-37.9

$$c = \varepsilon^2 c_2. \tag{5c}$$

From the chain rule of differentiation, the time derivatives in eqns (1) and (2) are transformed as $d(\)/dt = (d_0 + \varepsilon d_1 + \varepsilon^2 d_2 + \dots)(\)$, and $d^2(\)/dt^2 = (d_0^2 + 2\varepsilon d_0 d_1 + \varepsilon^2(d_1^2 + 2d_0 d_2) + \dots)(\)$, where $d_i^n(\) = \partial^n(\)/\partial t_i^n$.

In order to analyse the different resonant motions without losing the effect of the parametric excitation terms that appear on the right-hand sides of eqns (1) and (2), the quantities $f_v, f_{v\eta}, f_\theta$ and $f_{\theta\eta}$ will be treated as if they were independent of each other. For the primary resonance when the frequency of the external excitation, Ω , is near the natural frequency ω , for example, the excitation $f_v \cos(\Omega t)$ is taken out of the $O(\varepsilon)$ approximation by letting $f_v = \varepsilon^3 f_{v3}$ while all the other excitation terms are treated as $O(\varepsilon)$ in the analysis of this case.

SUPERHARMONIC RESONANCE WITH Ω NEAR $\sqrt{3}\omega_c/2$

Since the excitation frequency in this case is away from both ω and $\sqrt{3}\omega_c$, the forcing functions $f_v \cos(\Omega t)$ and $f_\theta \cos(\Omega t)$ in eqns (1) and (2) do not yield secular terms at $O(\varepsilon)$ and, therefore, are treated as $O(\varepsilon)$ quantities in the perturbation analysis. For this case we then write

$$f_v = \varepsilon f_{v1}, \quad f_\theta = \varepsilon f_{\theta1}, \quad f_{v\eta} = \varepsilon f_{v\eta1}, \quad f_{\theta\eta} = \varepsilon f_{\theta\eta1}. \tag{6}$$

By substituting eqns (5a-c) and (6) into the differential equations of motion, eqns (1) and (2), the following linear uncoupled partial differential equations are obtained at each level of approximation :

$O(\varepsilon)$

$$d_0^2 v_{i1} + \omega^2 v_{i1} = f_{v1} \cos(\Omega t_0), \tag{7a}$$

$$d_0^2 \theta_1 + 3\omega_c^2 \theta_1 = f_{\theta1} \cos(\Omega t_0); \tag{7b}$$

$O(\varepsilon^2)$

$$d_0^2 v_{i2} + \omega^2 v_{i2} = -2 d_0 d_1 v_{i1} - 2\omega_c^2(\beta_1 - 1)v_{i1} d_0 \theta_1, \tag{8a}$$

$$d_0^2 \theta_2 + 3\omega_c^2 \theta_2 = -2 d_0 d_1 \theta_1 + 12\omega_c^2(\beta_1 - 1) d_0(v_{i1}^2); \tag{8b}$$

$O(\varepsilon^3)$

$$d_0^2 v_{i3} + \omega^2 v_{i3} = -d_1^2 v_{i1} - 2 d_0 d_2 v_{i1} - 2 d_0 d_1 v_{i2} - c_2 d_0 v_{i1} - \beta_3 v_{i1}^3 - 2\omega_c(\beta_1 - 1)[v_{i1}(d_0 \theta_2 + d_1 \theta_1) + v_{i2} d_0 \theta_1] - (\beta_1 - 1)v_{i1}(d_0 \theta_1)^2 + 3\omega_c^2(\beta_1 + 1)v_{i1} \theta_1^2 - \beta_2 v_{i1} d_0^2(v_{i1}^2) + v_{i1}^2 f_{v\eta1} \cos(\Omega t_0), \tag{9a}$$

$$d_0^2 \theta_3 + 3\omega_c^2 \theta_3 = -d_1^2 \theta_1 - 2 d_0 d_2 \theta_1 - 2 d_0 d_1 \theta_2 + 12\omega_c(\beta_1 - 1)[d_1(v_{i1}^2) + 2 d_0(v_{i1} v_{i2})] + 2\omega_c^2 \theta_1^3 + 12\beta_1[v_{i1}^2(d_0^2 \theta_1 + 3\omega_c^2 \theta_1) + (d_0 \theta_1) d_0 v_{i1}^2] - 12 d_0(v_{i1}^2 d_0 \theta_1) + 36\omega_c^2 v_{i1}^2 \theta_1 + v_{i1}^2 f_{\theta\eta1} \cos(\Omega t_0). \tag{9b}$$

The solution to the $O(\varepsilon)$ differential equations is given by eqns (10a, b) below :

$$v_{i1} = A_v(t_1, t_2) \cos \phi_v + \frac{f_{v1}}{\omega^2 - \Omega^2} \cos \Omega t_0, \quad \phi_v = \omega t_0 + B_v(t_1, t_2), \tag{10a}$$

$$\theta_1 = A_\theta(t_1, t_2) \cos \phi_\theta + \frac{f_{\theta1}}{3\omega_c^2 - \Omega^2} \cos \Omega t_0, \quad \phi_\theta = \sqrt{3}\omega_c t_0 + B_\theta(t_1, t_2). \tag{10b}$$

After substituting the above solutions into eqns (8a, b), and defining a detuning $\varepsilon \sigma_1$ and a quantity $\gamma(t_1, t_2)$ as

$$\Omega = \frac{\sqrt{3}\omega_c}{2} (1 + \varepsilon\sigma_1), \tag{11a}$$

$$\gamma(t_1, t_2) = \sqrt{3}\omega_c\sigma_1 t_1 - B_\theta(t_1, t_2), \tag{11b}$$

the following conditions for elimination of secular terms [eqns (12a, b, c)] and particular solutions for v_{i2} and θ_2 [eqns (13a, b)] are obtained at the $O(\varepsilon^2)$ level:

$$d_1 A_v = d_1 B_v = 0, \tag{12a}$$

$$2\sqrt{3}\omega_c d_1 A_\theta + 12\Omega_c(1 - \beta_1) \frac{\Omega f_{v1}^2}{(\omega^2 - \Omega^2)^2} \cos \gamma = 0, \tag{12b}$$

$$2\sqrt{3}\omega_c A_\theta (\sqrt{3}\omega_c\sigma_1 - d_1\gamma) + 12\omega_c(1 - \beta_1) \frac{\Omega f_{v1}^2}{(\omega^2 - \Omega^2)^2} \sin \gamma = 0, \tag{12c}$$

$$\begin{aligned} v_{i2} = & \sqrt{3}(\beta_1 - 1)\omega_c^2 A_v A_\theta \left\{ \frac{\sin(\phi_v + \phi_\theta)}{\omega^2 - (\omega + \sqrt{3}\omega_c)^2} - \frac{\sin(\phi_v - \phi_\theta)}{\omega^2 - (\omega - \sqrt{3}\omega_c)^2} \right\} \\ & + \frac{(\beta_1 - 1)\omega_c \Omega A_v f_{\theta 1}}{3\omega_c^2 - \Omega^2} \left\{ \frac{\sin(\phi_v + \Omega t_0)}{\omega^2 - (\Omega + \omega)^2} - \frac{\sin(\phi_v - \Omega t_0)}{\omega^2 - (\Omega - \omega)^2} \right\} \\ & + \frac{\sqrt{3}(\beta_1 - 1)\omega_c^2 A_\theta f_{v1}}{\omega^2 - \Omega^2} \left\{ \frac{\sin(\phi_\theta + \Omega t_0)}{\omega^2 - (\sqrt{3}\omega_c + \Omega)^2} + \frac{\sin(\phi_\theta - \Omega t_0)}{\omega^2 - (\sqrt{3}\omega_c - \Omega)^2} \right\} \\ & + \frac{(\beta_1 - 1)\omega_c \Omega f_{v1} f_{\theta 1}}{(\omega^2 - \Omega^2)(3\omega_c^2 - \Omega^2)} \sin 2\Omega t_0, \end{aligned} \tag{13a}$$

$$\theta_2 = 12\omega_c(1 - \beta_1) A_v \left\{ \frac{\omega A_v \sin 2\phi_v}{3\omega_c^2 - 4\omega^2} + \frac{f_{v1} \sin(\phi_v + \Omega t_0)}{(\omega - \Omega)[3\omega_c^2 - (\omega + \Omega)^2]} + \frac{f_{v1} \sin(\phi_v - \Omega t_0)}{(\omega + \Omega)[3\omega_c^2 - (\omega - \Omega)^2]} \right\}. \tag{13b}$$

At the $O(\varepsilon^3)$ level, we now find that one of the conditions for elimination of the secular terms is obtained as

$$2d_2 A_v + c_2 A_v = 0. \tag{14}$$

Therefore, the first of eqns (12) and (14) disclose that the equilibrium solution for the bending motion corresponds to $A_v = 0$ and that this equilibrium is asymptotically stable. Thus, except for small higher harmonics, the bending motion is essentially given by the linear solution with an amplitude proportional to the excitation strength εf_{v1} as indicated by eqn (10a). For convenience in presentation, we will set $A_v = 0$ in the additional conditions for elimination of secular terms at the $O(\varepsilon^3)$ level. Such conditions are obtained as shown in eqns (15a, b) below:

$$2\sqrt{3}\omega_c d_2 A_\theta + 2(d_1 A_\theta)(\sqrt{3}\omega_c\sigma_1 - d_1\gamma) - A_\theta d_1^2 \gamma = 0, \tag{15a}$$

$$\begin{aligned} & 2A_\theta \sqrt{3}\omega_c d_2 \gamma + d_1^2 A_\theta - A_\theta (d_1 \gamma)^2 - 3A_\theta \omega_c^2 \left[\frac{A_\theta^2}{2} + \frac{16}{81} \left(\frac{f_{\theta 1}^2}{\omega_c^2} \right)^2 \right] \\ & - \omega_c^2 \underbrace{\frac{36}{(\omega^2 - \Omega^2)^2} \left\{ 1 + \omega_c^2(1 - \beta_1)^2 \left[\frac{1}{\omega^2 - (\sqrt{3}\omega_c + \Omega)^2} + \frac{1}{\omega^2 - (\sqrt{3}\omega_c - \Omega)^2} \right] \right\}}_{\approx 1.4 \times 10^{-4} (0 \leq \omega_c \leq 1), \quad 9.5 \times 10^{-3} (\omega_c = 5)} f_{v1}^2 A_\theta = 0. \end{aligned} \tag{15b}$$

By combining eqns (12) and (15), the following ordinary differential equations are finally obtained for the amplitude A_θ and phase γ of the $O(\varepsilon)$ solution for the pitch motion :

$$\dot{A}_\theta = \varepsilon d_1 A_\theta + \varepsilon^2 d_2 A_\theta + \dots = -\frac{\varepsilon \alpha_1}{2\sqrt{3}\omega_c} \left(1 - \frac{\varepsilon \sigma_1}{2}\right) f_{v1}^2 \cos \gamma, \tag{16a}$$

$$2\sqrt{3}\omega_c A_\theta \dot{\gamma} / \omega_c = 6\varepsilon \sigma_1 A_\theta + \varepsilon \alpha_1 \left(1 - \frac{\varepsilon \sigma_1}{2}\right) f_{v1}^2 \sin \gamma + \varepsilon^2 \left\{ 3A_\theta \left[\frac{A_\theta^2}{2} + \frac{16}{81} \left(\frac{f_{\theta 1}}{\omega_c^2}\right)^2 \right] + \alpha_2 A_\theta f_{v1}^2 \right\}, \tag{16b}$$

where

$$\alpha_1 = \frac{12(1 - \beta_1)\Omega}{(\omega^2 - \Omega^2)^2 \omega_c} \approx \frac{6(1 - \beta_1)}{(\omega^2 - 3\omega_c^2/4)^2}, \tag{17a}$$

$$\alpha_2 = \frac{36}{(\omega^2 - \Omega^2)^2} \left\{ 1 + \omega_c^2 (1 - \beta_1)^2 \left[\frac{1}{\omega^2 - (\sqrt{3}\omega_c + \Omega)^2} + \frac{1}{\omega^2 - (\sqrt{3}\omega_c - \Omega)^2} \right] \right\}. \tag{17b}$$

In eqns (17a, b), $\Omega \approx \sqrt{3}\omega_c/2$. For the first bending mode, one obtains $\alpha_1 \approx -8.2 \times 10^{-5}$ and $\alpha_2 \approx 1.4 \times 10^{-4}$ when $0 \leq \omega_c \leq 1$, and $\alpha_1 \approx -4.2 \times 10^{-5}$ and $\alpha_2 \approx 9.5 \times 10^{-5}$ when $\omega_c = 5$. The value of α_2 is also indicated in eqn (15b). The following amplitude-frequency relationship for the steady-state motion (i.e. $A_\theta = \text{constant} \triangleq A_{\theta c}$ and $\gamma = \text{constant} \triangleq \gamma_c = \pi/2$ and $-\pi/2$) is readily obtained from eqns (16a, b) :

$$6\varepsilon \sigma_1 \pm \frac{\alpha_1 (1 - \frac{1}{2}\varepsilon \sigma_1) (\varepsilon f_{v1})^2}{\varepsilon A_{\theta c}} + \varepsilon^2 \left[\frac{3}{2} A_{\theta c}^2 + \frac{16}{27} \left(\frac{f_{\theta 1}}{\omega_c^2}\right)^2 + \alpha_2 f_{v1}^2 \right] = 0. \tag{18}$$

The amplitude-frequency relationship that characterizes the superharmonic pitch motion is shown in Fig. 2 for $0 \leq \omega_c \leq 1$, $\varepsilon f_{v1}/(\omega^2 - \Omega^2) = 0.02$ ($\approx 10/22.373^2$) and the two values of $\varepsilon f_{\theta 1}/\omega_c^2$ indicated in that figure.

As indicated by eqns (10b) and (11a, b), the pitch motion for this case consists of an oscillation with amplitude equal to $4\varepsilon f_{\theta 1}/(9\omega_c^2)$, and frequency Ω , superimposed on an oscillation with amplitude $\varepsilon A_{\theta c}$ and frequency equal to 2Ω . The amplitude $\varepsilon A_{\theta c}$ of the component with frequency 2Ω depends on the nonlinearities and is determined by eqn (18).

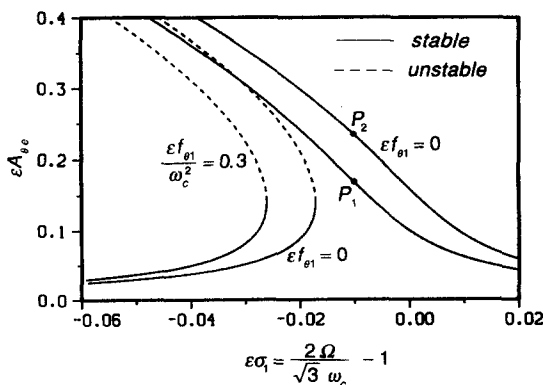


Fig. 2. Amplitude-frequency pitch response for Ω near $\sqrt{3}\omega_c/2$, with $0 \leq \omega_c \leq 1$ ($\omega \approx 22.373$) and $\varepsilon f_{v1}/(\omega^2 - 3\omega_c^2/4) = 0.02$ ($\approx 10/22.373^2$).

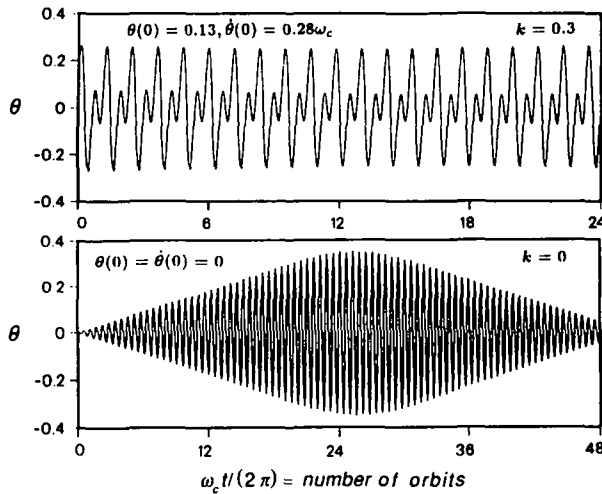


Fig. 3. Numerical integration of eqns (1) and (2) for Ω near $\sqrt{3}\omega_c/2$, with $\omega_c = 0.02$ ($\omega = 22.373$), $\varepsilon\sigma_1 = -0.01$, $\varepsilon^2c_2 = 0.1$, $v_i(0) = 0.02$, $\dot{v}_i(0) = 0$, and $E_\eta = 10F(s) + k\omega_c^2(s-1/2)$.

The component with frequency Ω is zero for excitations with $f_\theta = 0$. Figure 3 shows the undamped pitch motion obtained from the numerical integration of eqns (1) and (2) for $\omega_c = 0.02$ ($\omega = 22.373$), $\varepsilon^2c_2 = 0.1$, $\varepsilon\sigma_1 = -0.01$ and the excitation parameters corresponding to $E_\eta(s) = 10F(s) + k\omega_c^2(s-1/2)$ so that $f_v = 10$, $f_\theta = k\omega_c^2$, $f_{v\eta} = 449.6 - 12.3k\omega_c^2$ and $f_{\theta\eta} = -37.9k\omega_c^2$ (see Table 2). The response for $\omega_c = 1$ ($\omega = 22.577$) is virtually the same as that shown in Fig. 3, which was generated with $\omega_c = 0.02$. The initial conditions for $v_i(t)$ used in the numerical integration were $v_i(0) = 0.02$ and $\dot{v}_i(0) = 0$, which were chosen to correspond to the $O(\varepsilon)$ part of $v_i(t)$ given by eqn (10a) with $A_v = 0$. The upper part of Fig. 3 was obtained with $k = f_\theta/\omega_c^2 = 0.3$, and the initial conditions $\theta(0) = 0.13$ and $\dot{\theta}(0) = 0.28\omega_c$ (which correspond to point P_1 in Fig. 2). This undamped response just illustrates the superposition of the two frequency components in $\theta_1(t)$ given by eqn (10b). The lower portion of Fig. 3 was obtained with $f_\theta = \varepsilon f_{\theta 1} = 0$ and the initial conditions $\theta(0) = \dot{\theta}(0) = 0$ (which do not correspond to the steady-state response represented by point P_2 in Fig. 3). The slow modulation exhibited by that response is a result of the pitch motion being undamped and being started with initial conditions that do not correspond to the steady-state value of εA_{θ_c} determined from eqn (18) (and represented by the curve for $\varepsilon f_{\theta 1} = 0$ in Fig. 3). The pitch motion displayed in the lower portion of Fig. 3 repeats itself as time increases. Its amplitude, εA_θ , and phase γ , are governed by the differential equations (16a) and (16b). If the system had pitch damping, the pitch motion started with the initial conditions given above would have been, for $f_\theta = 0$, a steady motion whose amplitude would correspond to point P_2 in Fig. 3. As for the steady-state bending motion, except for the small higher harmonics, it consists of an oscillation of amplitude $\varepsilon f_{v1}/(\omega^2 - 3\omega_c^2/4) \approx 0.02$ and frequency Ω .

PRIMARY RESONANCE WITH Ω NEAR ω

To analyse this case we let

$$f_v = \varepsilon^3 f_{v3}, \quad f_\theta = \varepsilon f_{\theta 1}, \quad f_{v\eta} = \varepsilon f_{v\eta 1}, \quad f_{\theta\eta} = \varepsilon f_{\theta\eta 1}. \tag{19}$$

The solutions to the $O(\varepsilon)$ differential equations for this case are obtained as $v_{i1} = A_v(t_1, t_2) \cos[\omega t_0 + B_v(t_1, t_2)] \triangleq A_v \cos \phi_v$, and θ_1 as shown in eqn (10b) with $\Omega = \omega$ in that equation. The conditions for elimination of secular terms at the $O(\varepsilon^2)$ level now become:

$$d_1\alpha = 0 \quad \therefore \quad \alpha = \alpha(t_2), \quad \alpha = A_v, B_v, A_\theta, B_\theta. \quad (20)$$

The solutions for v_{t_2} and θ_2 are now obtained as shown in eqns (21a, b) given below. For later convenience, the homogeneous solution is included in the expression for θ_2 in order to transfer the initial conditions for the pitch motion to the $O(\varepsilon)$ approximation, thus making $\theta_2(t=0) = \dot{\theta}_2(t=0) = 0$:

$$v_{t_2} = (1 - \beta_1)\omega_c A_v \left\{ A_\theta \left[\frac{\sin(\phi_v + \phi_\theta)}{2\omega + \sqrt{3}\omega_c} + \frac{\sin(\phi_v - \phi_\theta)}{2\omega - \sqrt{3}\omega_c} \right] - \frac{f_{\theta 1}}{\omega(\omega^2 - 3\omega_c^2)} \left[\frac{\sin(\phi_v + \Omega t_0)}{3} + \sin(\phi_v - \Omega t_0) \right] \right\}, \quad (21a)$$

$$\theta_2 = K[A_v^2(t_2) \sin(2\phi_v) + C \cos \phi_\theta]. \quad (21b)$$

In eqn (21b), $K = 12(\beta_1 - 1)\omega_c\omega/(4\omega^2 - 3\omega_c^2)$ and C is a constant. For $0 \leq \omega_c \leq 1$ one obtains $K \approx 0.274\omega_c$ for the first mode.

To express the nearness of the excitation frequency to the bending natural frequency, a detuning parameter $\varepsilon^2\sigma_v$ is now introduced as

$$\Omega = \omega(1 + \varepsilon^2\sigma_v). \quad (22)$$

Substitution of the solution to the $O(\varepsilon)$ and $O(\varepsilon^2)$ equations into the $O(\varepsilon^3)$ differential equations, eqns (9a, b), yields a number of terms with frequencies ("measured" in the time scale t_0) equal to the natural frequencies of the system. In order to obtain a solution that is uniformly valid as $t \rightarrow \infty$, the coefficients of such resonant terms are equated to zero. This yields four differential equations for the variables $A_v(t_2)$, $B_v(t_2)$, $A_\theta(t_2)$ and $B_\theta(t_2)$. By defining a quantity $\gamma_v(t_2)$ as

$$\gamma_v(t_2) = \omega\sigma_v t_2 - B_v(t_2) \quad (23)$$

the following conditions for elimination of secular terms are obtained from eqns (9a, b):

$$\omega(2d_2A_v + c_2A_v) - [f_{v_3} + \frac{1}{4}f_{v\eta_1}A_v^2] \sin \gamma_v - \underbrace{\frac{1}{(\omega^2 - 3\omega_c^2)^2} \left[\frac{(\beta_1 - 1)\omega^2 + 3(\beta_1 + 1)\omega_c^2}{4} - (\beta_1 - 1)^2\omega_c^2 \right]}_{0.001(0 \leq \omega_c \leq 1), \quad 8.04 \times 10^{-4}(\omega_c = 5)} A_v f_{\theta 1}^2 \sin 2\gamma_v = 0, \quad (24a)$$

$$2\omega A_v(\omega\sigma_v - d_2\gamma_v) + [f_{v_3} + \frac{3}{4}f_{v\eta_1}A_v^2] \cos \gamma_v + 3\omega_c^2 \left[1 + \frac{2\omega_c^2(1 - \beta_1)^2}{4\omega^2 - 3\omega_c^2} \right] A_v A_\theta^2 + \left[\beta_2\omega^2 - \frac{3}{4}\beta_3 - \frac{24\omega_c^2\omega^2(1 - \beta_1)^2}{4\omega^2 - 3\omega_c^2} \right] A_v^3 + \underbrace{\frac{1}{(\omega^2 - 3\omega_c^2)^2} \left[\frac{(\beta_1 - 1)\omega^2 + 3(\beta_1 + 1)\omega_c^2}{4} - (\beta_1 - 1)^2\omega_c^2 \right]}_{0.001(0 \leq \omega_c \leq 1), \quad 8.04 \times 10^{-4}(\omega_c = 5)} A_v f_{\theta 1}^2 \cos 2\gamma_v - \underbrace{\frac{1}{(\omega^2 - 3\omega_c^2)^2} \left[\frac{(\beta_1 - 1)\omega^2 - 3(\beta_1 + 1)\omega_c^2}{2} - \frac{2(\beta_1 - 1)^2\omega_c^2}{3} \right]}_{0.002(0 \leq \omega_c \leq 1), \quad 0.0013(\omega_c = 5)} A_v f_{\theta 1}^2 = 0, \quad (24b)$$

$$d_2A_\theta = 0 \quad \therefore \quad A_\theta = \text{constant}, \quad (24c)$$

$$A_\theta \left\{ 2\sqrt{3}\omega_c d_2 B_\theta + \frac{3}{2}\omega_c^2 A_\theta^2 + 36\omega_c^2 \left[1 + \frac{2\omega_c^2(1-\beta_1)^2}{4\omega^2 - 3\omega_c^2} \right] A_v^2 + \frac{3\omega_c^2 f_{\theta 1}^2}{(\omega^2 - 3\omega_c^2)^2} \right\} = 0. \quad (24d)$$

The value of A_θ is determined by the initial conditions of the motion.

From the chain rule of differentiation, the time derivative of the quantities A_v, γ_v, A_θ and B_θ are obtained as $\dot{\alpha} = d\alpha/dt = \varepsilon d_1\alpha + \varepsilon^2 d_2\alpha + \dots = \varepsilon^2 d_2\alpha + \dots$ ($\alpha = A_v, \gamma_v, A_\theta, B_\theta$). Since these quantities do not depend on the time scale t_1 the differential equations for them are of the same form as eqns (24a–d). Those differential equations admit the equilibrium solution $A_v = \text{constant} \triangleq A_{ve}$ and $\gamma_v = \text{constant} \triangleq \gamma_{ve}$. An equilibrium solution to eqns (24a, b) corresponds to a steady-state periodic solution for the bending motion $v_{11}(t)$. Since the terms that are proportional to $f_{\theta 1}^2$ in those equations are each multiplied by a very small coefficient, their contribution to the equilibrium solution is very small. If it were not for the small effect of the parametric excitation term in eqns (24a, b), i.e. the terms proportional to $f_{v\eta 1} A_v^2$, those equations could also have been obtained by a simpler perturbation analysis by letting $E_\eta = O(\varepsilon^3)$ (i.e. with $f_v = \varepsilon^3 f_{v3}$ and $f_\theta = \varepsilon^3 f_{\theta 3}$). The small effect of the parametric excitation would have been lost in such analysis.

The amplitude–frequency relationship for the steady-state bending response of the beam is obtained by solving eqns (24a, b) numerically. If $f_{v\eta 1} A_{ve}^2/4 \ll f_{v3}$, the amplitude–frequency relationship for the harmonic response when Ω is near ω is essentially given as shown in eqn (25) below:

$$(\omega c_2)^2 + \underbrace{\left\{ 2\omega^2 \sigma_v + 3\omega_c^2 \left[1 + \frac{2\omega_c^2(1-\beta_1)^2}{4\omega^2 - 3\omega_c^2} \right] A_\theta^2 \right\}}_{\approx 3\omega_c^2(0 \leq \omega_c \leq 1), \quad 80.53(\omega_c = 5)} + \underbrace{\left\{ \beta_2\omega^2 - \frac{3}{4}\beta_3 - \frac{24\omega_c^2\omega^2(1-\beta_1)^2}{4\omega^2 - 3\omega_c^2} \right\} A_{ve}^2}_{\approx 1.5 \times 10^4(0 \leq \omega_c \leq 1), \quad 26,506(\omega_c = 5)} \approx \left(\frac{f_{v3}}{A_{ve}} \right)^2. \quad (25)$$

The values of the coefficients of A_θ^2 and A_{ve}^2 for the first mode, are indicated in eqn (25). Since the value of the coefficient of A_{ve}^2 is much higher than that for the coefficient of A_θ^2 , the amplitude–frequency response for the directly excited bending motion is essentially the same as the classical response of a Duffing oscillator with a softening nonlinearity. The small $f_{v\eta 1} A_{ve}^2$ and $A_{ve} f_{\theta 1}^2$ terms in eqns (24a, b) cause a small change in the response given by eqn (25) for the higher values of A_{ve} . Figure 4 shows the amplitude–frequency dependence for the bending response for $\varepsilon^2 c_2 = 0.05$, $\omega_c = 1$, $\omega = 22.577$, and the two values of $\varepsilon^3 f_{v3}$ indicated in the figure. The result shown in Fig. 4 was obtained by solving eqns (24a) and (24b) numerically with $A_v = A_{ve}$ and $\gamma = \gamma_{ve}$. The amplitude–frequency response curves for $0 \leq \omega_c \leq 1$ are essentially indistinguishable from those shown in Fig. 4, while those for

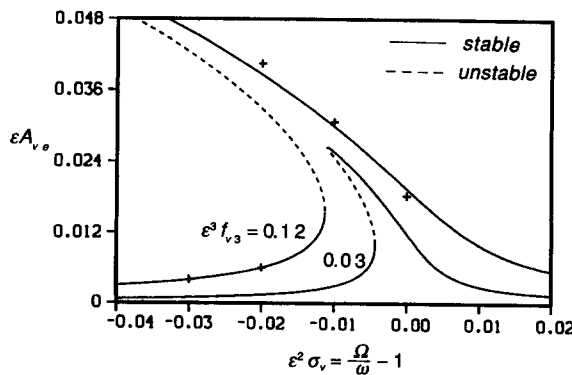


Fig. 4. Amplitude–frequency bending response for Ω near ω , with $\omega_c = 1$, $\omega = 22.577$ (or $0 \leq \omega_c \leq 1$) and $\varepsilon^2 c_2 = 0.05$.

higher values of ω_c are similar to those shown in that figure. The maximum amplitude of the bending response determined from eqn (25) is equal to $\varepsilon^3 f_{r3}/(\omega \varepsilon^2 c_2)$. The value of the maximum amplitude (and, thus, of the frequency where the jump phenomenon occurs) is slightly affected by the small terms discussed above. By decreasing the value of the strength of the excitation, $\varepsilon^3 f_{r3}$, one can “shrink” the plots shown in that figure and eventually eliminate the jump phenomenon so that the response more closely resembles the linear response. The points marked with a cross in that figure represent the result of the numerical integration of eqns (1) and (2) with the values of f_θ , $f_{v\eta}$ and $f_{\theta\eta}$ corresponding to $E_\eta(s) = 0.12F(s)$ (see Table 2).

The steady-state v -motion for the case considered in this section is essentially an oscillation with frequency Ω given as $v = \varepsilon A_{ve} \cos(\Omega t - \gamma_{ve}) + O(\varepsilon^2)$, with A_{ve} determined from eqns (24a, b), or from Fig. 4 for the values of the parameters shown in that figure. In contrast, the undamped θ -motion depends on initial conditions and on the v -motion. After the v -motion reaches its steady state, the θ -motion is given as

$$\theta = \varepsilon A_\theta \cos \phi_\theta + K[(\varepsilon A_{ve})^2 \sin 2(\Omega t - \gamma_{ve}) + \varepsilon^2 C \cos \phi_\theta] + O(\varepsilon^3), \tag{26}$$

with $\phi_\theta = \omega_\theta^* t + B_{\theta 0}$, where $B_{\theta 0}$ is a constant and the frequency ω_θ^* is determined as

$$\omega_\theta^* = \sqrt{3\omega_c} \left\{ 1 - \frac{(\varepsilon A_\theta)^2}{4} - 6 \left[1 + \frac{2\omega_c^2(1 - \beta_1)^2}{4\omega^2 - 3\omega_c^2} \right] (\varepsilon A_{ve})^2 - \frac{(\varepsilon f_{\theta 1})^2}{2(\omega^2 - 3\omega_c^2)^2} \right\} + O(\varepsilon^2). \tag{27}$$

The $O(\varepsilon^2)$ part of the pitch motion given by eqn (26) consists of a component with frequency 2Ω , whose amplitude is proportional to the square of the amplitude of the steady-state bending motion, and a component with frequency ω_θ^* , whose amplitude is equal to $\varepsilon^2 C$. By imposing the condition $\theta_2(0) = \dot{\theta}_2(0) = 0$, the constant $\varepsilon^2 C$ is obtained as

$$\varepsilon^2 C = \pm 2 \sqrt{\left(\frac{v_0 \dot{v}_0}{\omega} \right)^2 + \left(\frac{\omega}{\sqrt{3\omega_c}} \right)^2 \left[v_0^2 - \left(\frac{\dot{v}_0}{\omega} \right)^2 \right]^2}, \tag{28}$$

where $v_0 = v_t(0)$ and $\dot{v}_0 = \dot{v}_t(0)$. Thus, the pitch motion depends not only on the steady-state amplitude of the bending motion, but also on the initial conditions for the bending and pitch motions of the beam. For the special case when $A_\theta = 0$, for example, which corresponds to $\theta(0) = \dot{\theta}(0) = 0$, the resulting pitch motion depends on the bending motion only. If, in addition to having $A_\theta = 0$, the bending motion is started with $\dot{v}_t(0) = 0$, the resulting pitch motion is given as

$$\theta(t) = K \left[(\varepsilon A_{ve})^2 \sin 2\Omega t - \frac{2\omega}{\sqrt{3\omega_c}} \varepsilon^2 v_{t1}^2(0) \sin \omega_\theta^* t \right] + O(\varepsilon^3).$$

For the cases when $2\omega v_t^2(0)/(\sqrt{3\omega_c}) \gg (\varepsilon A_{ve})^2$, the steady-state pitch motion consists essentially of an oscillation of frequency ω_θ^* whose amplitude is proportional to the square of the initial amplitude of the fast-oscillating flexural motion. For such cases, the amplitude of the steady-state pitch motion corresponding to the first bending mode is approximately equal to $2K\omega v_0^2/(\sqrt{3\omega_c}) \approx 7.1v_0^2$ when $0 \leq \omega_c \leq 1$. Numerical integration of eqns (1) and (2) confirmed these results. The resulting bending motion for this case is essentially a sinusoid as described above. As $v_t(0)$ approaches zero, the $O(\varepsilon^2)$ component in eqn (26), with frequency 2Ω , and the higher order components, start to affect the very small resulting motion, which will then consist of a high frequency oscillation with frequency 2Ω whose amplitude is modulated by lower frequency higher order components.

PRIMARY RESONANCE WITH Ω NEAR $\sqrt{3}\omega_c$

The motion for this case is analysed by letting

$$f_\theta = \varepsilon^3 f_{\theta 3}, \quad f_v = \varepsilon f_{v1}, \quad f_{v\eta} = \varepsilon f_{v\eta 1}, \quad f_{\theta\eta} = \varepsilon f_{\theta\eta 1}, \quad (29)$$

and the solution to the $O(\varepsilon)$ differential equations are now obtained as shown in eqns (30a, b):

$$v_{r1} = A_v(t_1, t_2) \cos [\omega t_0 + B_v(t_1, t_2)] + \frac{f_{v1}}{\omega^2 - \Omega^2} \cos \Omega t_0 \triangleq A_v \cos \phi_v + K_v \cos \Omega t_0, \quad (30a)$$

$$\theta_1 = A_\theta(t_1, t_2) \cos [\sqrt{3}\omega_c t_0 + B_\theta(t_1, t_2)] \triangleq A_\theta \cos \phi_\theta. \quad (30b)$$

The conditions for elimination of secular terms in this case are the same as in eqn (20) and the solution to the $O(\varepsilon^2)$ differential equations are the same as in eqn (13a) and (13b), with $f_{\theta 1} = 0$ in those equations.

At the $O(\varepsilon^3)$ level, we also find that one of the conditions for elimination of the secular terms is obtained as

$$2 d_2 A_v + c_2 A_v = 0. \quad (31)$$

Thus, as in the superharmonic resonance with Ω near $\sqrt{3}\omega_c/2$, $A_v \rightarrow 0$ as $t \rightarrow \infty$, and the $O(\varepsilon)$ solution for the bending motion consists only of the particular solution due to the external excitation.

By expressing the nearness of Ω to $\sqrt{3}\omega_c$ as

$$\Omega = \sqrt{3}\omega_c(1 + \varepsilon^2 \sigma_\theta) \quad (32)$$

and by defining a quantity $\gamma_\theta(t_2)$ as

$$\gamma_\theta(t_2) = \sqrt{3}\omega_c \sigma_\theta t_2 - B_\theta(t_2) \quad (33)$$

the conditions for elimination of secular terms in the $O(\varepsilon^3)$ differential equations are obtained as shown in eqns (34a, b) below:

$$2\sqrt{3}\omega_c d_2 A_\theta - \alpha_4 A_\theta f_{v1}^2 \sin 2\gamma_\theta - [f_{\theta 3} + \alpha_5 f_{\theta\eta 1} f_{v1}^2] \sin \gamma_\theta = 0, \quad (34a)$$

$$2\sqrt{3}A_\theta(\sqrt{3}\omega_c \sigma_\theta - d_2 \gamma_\theta)/\omega_c + \frac{3}{2}A_\theta^3 + [\alpha_3 + \alpha_4 \cos 2\gamma_\theta]A_\theta f_{v1}^2 + [(f_{\theta 3} + \alpha_5 f_{\theta\eta 1} f_{v1}^2)/\omega_c^2] \cos \gamma_\theta = 0, \quad (34b)$$

where

$$\alpha_3 = \frac{36}{(\omega^2 - 3\omega_c^2)^2} \left\{ 1 + \omega_c^2(\beta_1 - 1)^2 \left[\frac{1}{\omega^2 - 12\omega_c^2} + \frac{1}{\omega^2} \right] \right\}, \quad (35a)$$

$$\alpha_4 = \frac{18}{(\omega^2 - 3\omega_c^2)^2} \left[\beta_1 - \frac{2\omega_c^2(\beta_1 - 1)^2}{\omega^2} \right], \quad (35b)$$

$$\alpha_5 = \frac{3}{4(\omega^2 - 3\omega_c^2)^2}. \quad (35c)$$

For the first mode one obtains $\alpha_3 \approx 1.43 \times 10^{-4}$, $\alpha_4 \approx 2.19 \times 10^{-4}$ and $\alpha_5 \approx 2.92 \times 10^{-6}$ when $0 \leq \omega_c \leq 1$, and $\alpha_3 = 1.167 \times 10^{-4}$, $\alpha_4 = 1.16 \times 10^{-4}$ and $\alpha_5 = 1.753 \times 10^{-6}$ when $\omega_c = 5$.

Equations (34a, b) admit the following equilibrium solutions, which correspond to $A_\theta = \text{constant} \triangleq A_{\theta c}$ and $\gamma_\theta = \text{constant} \triangleq \gamma_{\theta c}$.

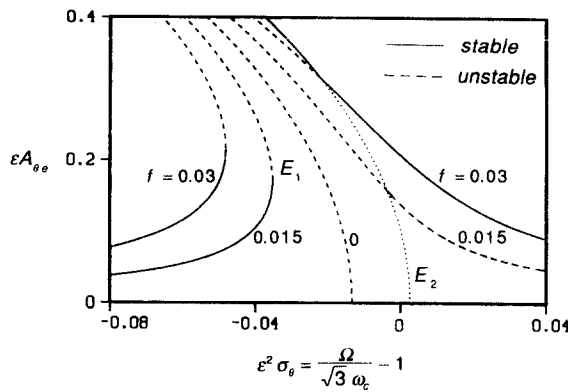


Fig. 5. Amplitude–frequency pitch response for Ω near $\sqrt{3}\omega_c$, with $\omega_c = 1$ (or $0 \leq \omega_c \leq 1$), $\omega = 22.577$, $f_v = 15$, and several values of $f \triangleq (f_0 + \alpha_5 f_v^2 f_{\theta\eta})/\omega_c^2$.

Equilibrium E_1

$$\sin \gamma_{\theta c} = 0 \quad \therefore \quad \cos \gamma_{\theta c} = \pm 1, \tag{36a}$$

$$\sigma_\theta = -\frac{1}{4}A_{\theta c}^2 - \frac{\alpha_3 + \alpha_4}{6} f_{v1}^2 \pm \frac{f_{\theta 3} + \alpha_5 f_{\theta\eta 1} f_{v1}^2}{6\omega_c^2 A_{\theta c}}. \tag{36b}$$

Equilibrium E_2

$$\cos \gamma_{\theta c} = -\frac{1}{A_{\theta c}} \left[\frac{f_{\theta 3}}{2\alpha_4 f_{v1}^2} + \frac{\alpha_5}{2\alpha_4} f_{\theta\eta 1} \right], \tag{37a}$$

$$\sigma_\theta = -\frac{1}{4}A_{\theta c}^2 + \frac{\alpha_4 - \alpha_3}{6} f_{v1}^2. \tag{37b}$$

The pitch amplitude–frequency response curves for the equilibrium solutions E_1 and E_2 given by eqns (36b) and (37b) are shown in Fig. 5 for $\omega_c = 1$, $\omega = 22.577$ (first bending mode), $f_v = 15$ and several values of the parameter $f \triangleq (f_0 + \alpha_5 f_v^2 f_{\theta\eta})/\omega_c^2$. The stable and unstable parts of the responses are identified in that figure. Equilibrium E_2 exists only in the region where the values of $|\cos \gamma_\theta|$, determined from eqn (37a), are not greater than unity. The region where E_2 does not exist is indicated by a dotted line in Fig. 5 when $f = 0.03$. For $f = 0.015$, for example, E_2 does not exist when $\varepsilon A_{\theta c} < 0.16$ (which corresponds to the intersection of one of the curves for equilibrium E_1 for $f = 0.015$ with the E_2 curve shown in Fig. 5). In Fig. 6 the steady-state amplitude of the pitch response for E_1 and E_2 is shown plotted versus the parameter f_v for $f = 0.02$ and several values of the frequency detuning $\varepsilon^2 \sigma_\theta$. The dotted line indicates the region where equilibrium E_2 does not exist. As

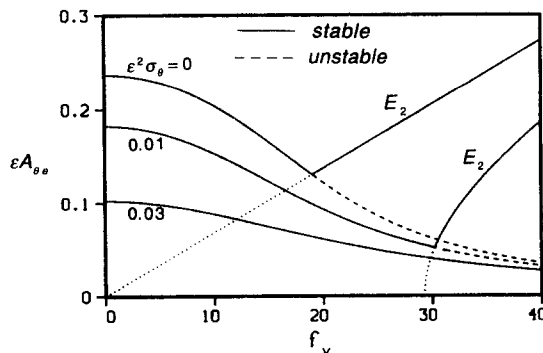


Fig. 6. Steady-state pitch amplitude versus f_v for Ω near $\sqrt{3}\omega_c$, with $\omega_c = 1$, $\omega = 22.577$ (or $0 \leq \omega_c \leq 1$), $f = 0.02$ and several values of $\varepsilon^2 \sigma_\theta$.

shown in Fig. 6, the steady-state pitch response is given by equilibrium E_1 for the smaller values of f_v . As f_v is increased, one reaches a critical value of f_v above which E_1 becomes unstable and the response is then determined by eqn (37b) for equilibrium E_2 . Along the curve marked E_2 the pitch response is insensitive to the excitation parameter f_θ that appears on the right-hand side of eqn (2).

The steady-state pitch amplitude–frequency response characteristics for equilibrium E_1 shown in Fig. 5 are essentially the same as those for an undamped Duffing oscillator with a softening nonlinearity while the steady-state response for equilibrium E_2 , which is independent of the excitation parameters appearing in eqn (2), is characteristic of a parametrically excited Duffing oscillator.

In order to further investigate the effect any bending motion has on pitch, consider the special case when the excitation distribution $E_\eta(s)$ is such as to yield $f_\theta = 0$ and that $f_{\theta\eta}$ is also nearly zero. In this case, the differential equations for A_θ and γ_θ , obtained from eqns (34a, b), may be written as follows:

$$\sqrt{3}(A_\theta^2)'/\omega_c = \varepsilon^2 \alpha_4 A_\theta^2 f_{v1}^2 \sin 2\gamma_\theta, \tag{38a}$$

$$2\sqrt{3}A_\theta \dot{\gamma}_\theta / \omega_c = \varepsilon^2 A_\theta [6\sigma_\theta + \frac{3}{2}A_\theta^2 + (\alpha_3 + \alpha_4 \cos 2\gamma_\theta) f_{v1}^2]. \tag{38b}$$

By multiplying eqn (38a) by the expression given by the right-hand side of eqn (38b), and eqn (38b) by the right-hand side of eqn (38a), the following integral of motion is readily obtained from the resulting differential equation:

$$3A_\theta^2(2\sigma_\theta + \frac{1}{4}A_\theta^2) + f_{v1}^2(\alpha_3 + \alpha_4 \cos 2\gamma_\theta)A_\theta^2 = \text{constant} \triangleq H. \tag{39}$$

By solving eqn (39) for $\cos 2\gamma_\theta$, the following differential equation governing the amplitude A_θ for the first order approximation for the pitch motion is readily obtained:

$$\sqrt{3}(A_\theta^2)'/\omega_c = \pm \varepsilon^2 f_{v1}^2 A_\theta^2 \sqrt{\alpha_4^2 - \left[\frac{H/A_\theta^2 - 3(2\sigma_\theta + A_\theta^2/4)}{f_{v1}^2} - \alpha_3 \right]^2} \triangleq \pm \varepsilon^2 f_{v1}^2 A_\theta^2 \sqrt{g(A_\theta^2)}. \tag{40}$$

The integral of the motion for eqn (40), given by eqn (39), provides the condition under which energy is exchanged between the bending and pitch motions of the beam when the only excitation is the term $f_v \cos(\Omega t)$ in eqn (1). The nonlinear phenomenon represented by eqn (40) occurs when $g(A_\theta^2) \geq 0$, and the extremum values of A_θ correspond to $g(A_\theta^2) = 0$. Of special interest is the case for which the pitch motion is started with very small initial conditions $\theta(0)$ and $\dot{\theta}(0)$ so that $H \approx 0$. For this case the function $g(A_\theta^2)$ reduces to

$$g(A_\theta^2) = \frac{9}{16f_{v1}^4} (A_{m\theta 1}^2 - A_\theta^2)(A_\theta^2 - A_{m\theta 2}^2), \tag{41a}$$

where

$$A_{m\theta 1}^2 = -\frac{4(\alpha_4 + \alpha_3)f_{v1}^2}{3} - 8\sigma_\theta, \tag{41b}$$

$$A_{m\theta 2}^2 = \frac{4(\alpha_4 - \alpha_3)f_{v1}^2}{3} - 8\sigma_\theta \triangleq A_{\theta_{\max}}^2. \tag{41c}$$

The quantities $A_{\theta m 1}^2$ and $A_{\theta m 2}^2$ are the roots of the polynomial $g(A_\theta^2)$. The root $A_{\theta m 1}^2$ becomes zero when $\sigma_\theta = \sigma_{\theta 1}$ while the root $A_{\theta m 2}^2$ is zero when $\sigma_\theta = \sigma_{\theta 2}$ where

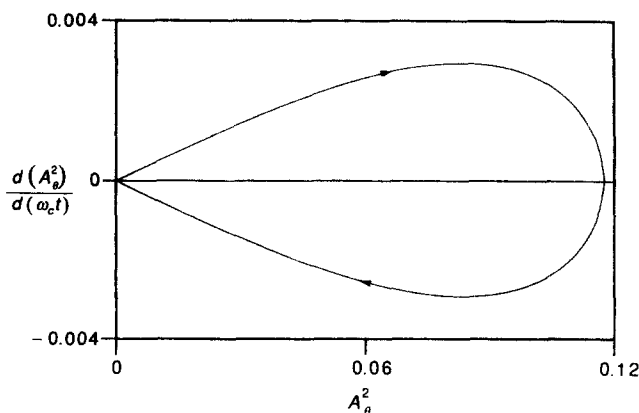


Fig. 7. Phase plane trajectory associated with eqn (40).

$$\sigma_{\theta 1} = \sigma_{\theta}(A_{\theta m 1}^2 = 0) = -\frac{(\alpha_4 + \alpha_3)f_{v1}^2}{6}, \tag{42a}$$

$$\sigma_{\theta 2} = \sigma_{\theta}(A_{\theta m 2}^2 = 0) = \frac{(\alpha_4 - \alpha_3)f_{v1}^2}{6}. \tag{42b}$$

With both α_3 and α_4 greater than zero, and $\alpha_4 > \alpha_3$, it follows that $\sigma_{\theta 1} < 0$ and $\sigma_{\theta 2} > 0$. When $\varepsilon^2\sigma_{\theta 1} < \varepsilon^2\sigma_{\theta} < \varepsilon^2\sigma_{\theta 2}$, the function $g(A_{\theta}^2)$ is positive and, therefore, the amplitude of the pitch motion $\theta(t) \approx \varepsilon\theta_1(t)$ grows to a large value which is equal to $\varepsilon A_{\theta \max}$. As disclosed by eqn (41c), the maximum value $\varepsilon A_{\theta \max}$ of the pitch motion in this region of resonance is independent of the initial conditions in pitch. This is illustrated by the phase plane trajectory associated with eqn (40); shown in Fig. 7.

The maximum amplitude of the resonant pitch motion can be readily determined by making use of Fig. 8, for which $0 \leq \omega_c \leq 1$. Each straight line corresponding to a particular value of f_v in that figure is given by eqn (41c). For a given value of f_v , the upper bound for the frequency detuning for a resonant motion to occur, $\varepsilon^2\sigma_{\theta 2}$, is determined by the intersection of the corresponding straight line \mathcal{L} with the $\varepsilon^2\sigma_{\theta}$ axis. The lower bound $\varepsilon^2\sigma_{\theta 1}$ for the detuning $\varepsilon^2\sigma_{\theta}$ is determined by the intersection of line \mathcal{L} with the straight line $A_{\theta \max}^2$ ($\sigma_{\theta} = \sigma_{\theta 1}$) = $-16\sigma_{\theta}/(1 + \alpha_3/\alpha_4)$. The lower boundary of the resonant region in the space $\varepsilon^2 A_{\theta \max}^2, \varepsilon^2\sigma_{\theta}$ is indicated by the dashed line in Fig. 8. The region of resonance in the space $(f_v^2, \varepsilon^2\sigma_{\theta})$ is shown in Fig. 9 for $0 \leq \omega_c \leq 1$. Figure 10 shows the pitch motion obtained by

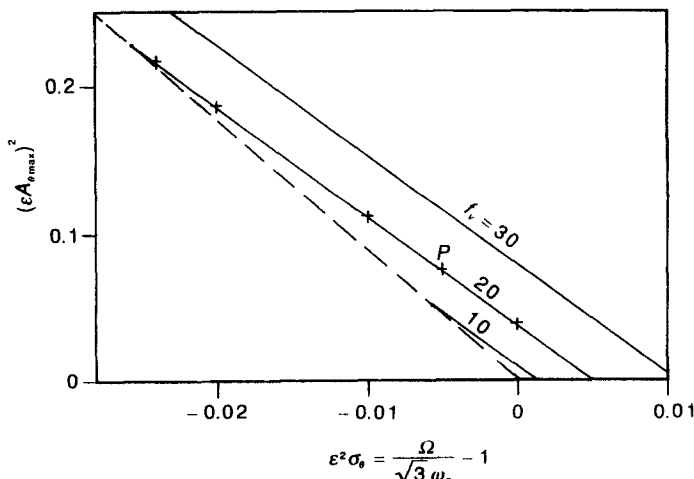


Fig. 8. $(\varepsilon A_{\theta \max})^2$ versus $\varepsilon^2\sigma_{\theta}$ for Ω near $\sqrt{3}\omega_c$, with $\omega_c = 1$ and $\omega = 22.577$ (or $0 \leq \omega_c \leq 1$).

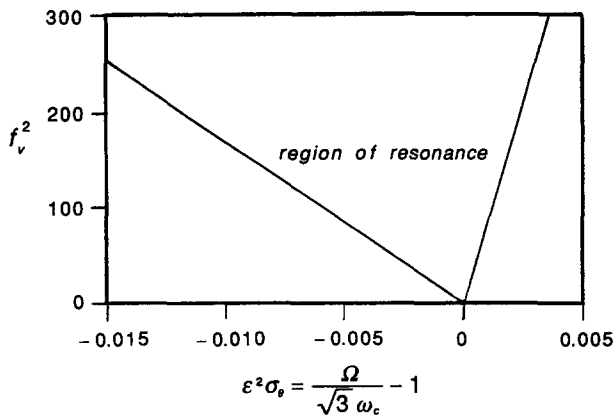


Fig. 9. The region of resonance in the $(f_v^2, \epsilon^2\sigma_\theta)$ parameter space for the first bending mode and for $0 \leq \omega_c \leq 1$.

numerical integration of eqns (1) and (2) with $v_i(0) = \dot{v}_i(0) = \dot{\theta}(0) = 0$, $\theta(0) = 0.05$, $\omega_c = 0.02$, $\omega = 22.373$ and $E_\eta(s) = 20F(s)$ (the values of the excitation parameters can be obtained from those listed in Table 2). The steady-state bending motion is essentially sinusoidal with amplitude equal to $f_v/(\omega^2 - 3\omega_c^2) \approx 0.04$, as predicted by eqn (30a) with $A_v = 0$. The motion depicted in the upper part of the figure shows a resonant motion for which $\epsilon^2\sigma_\theta = -0.005$. For this case, if $\theta(0)$ is reduced, the envelope of the pitch motion still reaches the same peak value $\theta_{max} \approx 0.28$, although it takes longer to reach that value. The lower part of Fig. 10 shows the pitch motion for $\epsilon^2\sigma_\theta = -0.03$, which is a value outside the region of resonance. Such motion is now dependent on the pitch initial conditions. This is confirmed by numerical integration of eqns (1) and (2). The maximum amplitude of the resonant pitch motion shown in the upper part of Fig. 10 corresponds to the point marked *P* in Fig. 8. The other points marked in Fig. 8 show the result of the numerical integration of eqns (1) and (2). These figures clearly disclose the excellent agreement with the results predicted by the analysis presented in this paper. The half period of the envelope of the resonant pitch motion shown in Fig. 10 may also be estimated by integrating eqn (40).

SUMMARY

The nonlinear differential equations of motion formulated by the authors (Crespo da Silva and Zaretsky, 1993) and expanded to contain up to third order polynomial non-

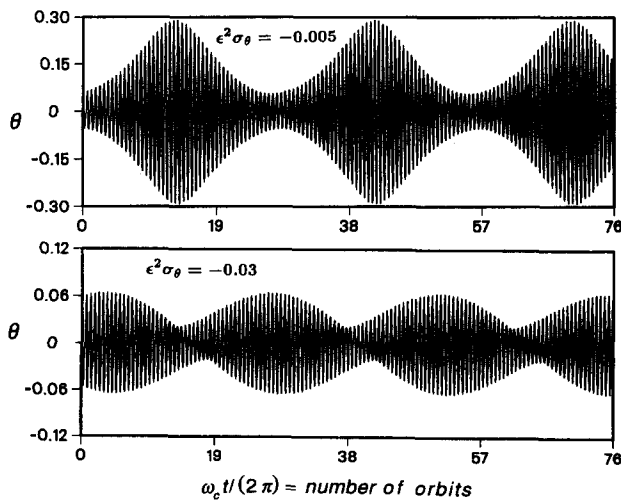


Fig. 10. Numerical integration of eqns (1) and (2) for Ω near $\sqrt{3}\omega_c$, with $\omega_c = 0.02$ ($\omega = 22.373$), $\epsilon^2c_2 = 0.1$, $v_i(0) = 0$, $\dot{v}_i(0) = 0$, $\theta(0) = 0.05$, $\dot{\theta}(0) = 0$, $f_v = 20$, $f_\theta = 0$, $f_{\eta_1} = 899.2$ and $f_{\eta_2} = 0$.

linearities have been applied to study the resonant coupled planar flexural-pitching motions of a beam in circular orbit about a massive central attracting body. The nonlinearities in the equations are due to nonlinear curvature and inertial effects, coupling between the bending and pitch motions, and contributions from the gravity gradient moment.

Three types of resonances have been considered. For the superharmonic pitch resonance it was found that the first approximation for the pitch response consists of two harmonic components, with the amplitude of one of the components being affected by the nonlinearities. For the primary bending resonance it was determined that while the amplitude-frequency response of the bending motion is characteristic of a classical Duffing oscillator, the pitch component of the response consists of a low frequency oscillation whose amplitude is dependent on initial conditions and a higher frequency component whose amplitude is dependent on the steady-state bending amplitude. For the primary pitch resonance the pitch response was shown to exhibit characteristics of a Duffing oscillator with a softening nonlinearity and a parametrically excited Duffing oscillator. It was also found that if the pitch motion is started with small initial conditions within a certain region in the space $(f_v^2, \varepsilon^2 \sigma_\theta)$ the pitch motion will grow to a maximum value which is independent of the pitch initial conditions.

REFERENCES

- Crespo da Silva, M. R. M. and Zaretzky, C. L. (1993). Nonlinear dynamics of a flexible beam in a central gravitational field—I. Equations of motion. *Int. J. Solids Structures* **30**, 2287–2299.
- Crespo da Silva, M. R. M., Zaretzky, C. L. and Hodges, D. H. (1991). Effects of approximations on the static and dynamic response of a cantilever with a tip mass. *Int. J. Solids Structures* **27**, 565–583.
- Nayfeh, A. H. and Mook, D. T. (1989). *Nonlinear Oscillations*. Wiley Interscience, New York.